7324 *Macromolecules* **2009**, *42*, 7324–7331
DOI: 10.1021/ma901090r

Macromolecules
ARTICLE

Shape Memory Polymers Based on Naturally-Occurring Bile Acids

Julien E. Gautrot and X. X. Zhu*

Département de chimie, Université de Montréal, C.P. 6128, succursale Centre-ville, Montréal, Québec, H3C 3J7, Canada

Received May 19, 2009; Revised Manuscript Received September 1, 2009

ABSTRACT: Naturally occurring bile acids are ideal building blocks for a new generation of biomaterials displaying low systemic toxicity and engineered properties. Herein we report the synthesis of bile acid-based polyesters using entropy-driven ring-opening metathesis polymerization (ED-ROMP) and characterization of the structure of the resulting polymers. The materials synthesized display high molecular weights (M_n above 100000), typical of ED-ROMPs. The mechanical and responsive behavior of these bile acid-based polyesters (BAPs) is studied by dynamic mechanical analysis (DMA) and thermomechanical cycling. Although BAPs are amorphous thermoplastics, they display typical rubber-like elasticity with tunable mechanical behavior, glass transitions close to body temperature, and outstanding shape memory properties. By introducing small changes in the chemical structure of BAPs (amide bonds or additional hydroxyl groups), we were able to correlate the materials' stiffness, their T_g and shape recovery temperature to their structure. In addition, we show that BAPs can be deformed to high strains even at low temperature and still display shape recovery.

Introduction

Shape memory materials commonly used for biomedical applications are typically based on alloys such as nitinol.[1] The biocompatibility of these alloys is well documented and their shape memory performance exceptional, but their high Young's modulus (tens of GPa) and permanent character upon implantation are sometimes seen as limitations to their use with soft tissues. Shape memory polymers (SMPs) are promising substitutes for alloys.[2−6] They display lower Young's moduli (considerably reducing the compliance mismatch at the device/tissue interface) and potential degradability. Typical SMPs include polyurethanes,[5] polyaramides,[7] polyesters[8] and, in most cases, shape recovery is triggered by a melting transition. Considering the intense research effort devoted to the study of polymer scaffolds for tissue engineering and drug release, SMPs are attractive responsive materials for regenerative medicine. SMPs would ideally present a bioactive surface and degrade in a controlled fashion in vivo into nontoxic compounds while releasing suitable cues stimulating tissue regeneration. Reports have proposed the use of SMPs as smart suture materials[4] and responsive stents for cardiovascular engineering.[9,10] However, materials displaying an optimal combination of well-matched mechanical properties, shape memory effect, and bioactivity still remain elusive.

Bile acids are naturally occurring molecules biosynthesized from cholesterol and are present in relatively large quantities in the human body, which produces half a gram of these compounds daily. They possess key features for biopolymer design: (i) upon degradation, materials based on these compounds would elicit little systemic toxicity; (ii) their high molecular weight and pK_a[11] contrast with that of small aliphatic molecules (e.g., lactic acid or ε-caprolactone), which typically give rise to pH drops upon degradation of their corresponding polyesters, often triggering inflammation and necrosis;[12] (iii) bile acids offer well-controlled chemistries and facial amphiphilicity, which make them ideal building blocks for drug delivery and sequestration systems.[13,14]

The incorporation of a bile acid (or steroidal) moiety within the main backbone of a macromolecule has remained a challenge until very recently. It was recognized that, although the large size of the steroidal structure does not allow the formation of strained cycles (as in lactides, ε-caprolactone and norbornene), which typically undergo ring-opening polymerization (ROP), unstrained macrocycles can also be ring-opened. In such cases, entropy drives the polymerization. Although no strain energy is stored in the structure of flexible macrocycles, their opening and subsequent increase of conformational freedom gives rise to a substantial entropy gain. As a result, entropy-driven ROP (ED-ROP) does not release any heat or evolve volatile molecules, which makes it suitable for micromolding and in situ polymerization.[15]

ED-ROP has been demonstrated for coordination/insertion,[16] enzymatic,[17] anionic,[18] and metathesis[19] polymerizations. Among these, the metathesis of alkenes has proven the most versatile, owing to the good reactivity, stability and chemoselectivity of ruthenium-based catalysts. It was recently demonstrated that ring-opening metathesis polymerization (ROMP) of fully aliphatic, mixed aliphatic-aromatic and aliphatic-steroidal macrocycles can afford high molecular weight materials (up to hundreds of kDa) very quickly (in a few minutes).[19−22] The high degree of polymerization achieved via such methods confers to the materials mechanical stability and strength. This concept was applied to the synthesis of bile acid-based polyesters (BAPs) and led to materials displaying elastomeric properties with Young's moduli near 1−2 MPa at 37 °C, which make them suitable for soft tissue engineering.[21,23,24]

Herein we report the high-performance shape memory properties of BAPs, both in the warm and cold drawing modes. We also extend this new family of polymers to mono- and bis-amides, as well as cholic acid, and draw structure−property relationships. In particular, we show that the transition temperature at which the shape recovery occurs can be predicted precisely and fine-tuned (e.g., to the body temperature) in view of a particular application.

*To whom correspondence should be addressed. E-mail: julian.zhu@umontreal.ca.

 Published on Web 09/18/2009

Experimental Section

Reagents. Lithocholic acid, cholic acid, ω-undecenoyl chloride, triethyl amine, ricinoleic acid, dicyclohexylcarbodiimide, 4-(dimethylamino)-pyridine, benzylidene-bis(tricyclohexylphosphine) dichlororuthenium (Grubbs' catalyst first generation), and [1,3-bis-(2,4,6-trimethylphenyl)-2-imidazolidinylidene)dichloro-(phenylmethylene)-(tricyclohexylphosphine)ruthenium] (Grubbs' catalyst second generation) were purchased from Aldrich (purest grade available from this supplier) and solvents from VWR. Dichloromethane (DCM) was dried using a solvent purification system from Glass Contour. Silica gel 230−400 mesh for chromatography was purchased from Qingdao Meicao Co., China. Tetrahydrofuran (THF) for SEC was filtered using white nylon 0.2 μm Millipore filters. Cyclic oligomers **3**[25] and polymers **1a** and **b**[21] were synthesized following methods reported in the literature.

Instruments. Thermogravimetric analyses (TGA) were performed on a Hi-Res TGA 2950 thermogravimetric analyzer (TA Instruments, measurement in air; T_{dec} was defined as the onset of decomposition temperature). Differential scanning calorimetry (DSC) measurements were carried out on a DSC 2910 differential scanning calorimeter from TA Instruments (heating rate was 10 °C/min and T_g was defined as the inflection point in the change of heat capacity). IR spectra were recorded on an Excalibur HE series FTS 3100 instrument from Digilab. ^{1}H and ^{13}C NMR spectra were recorded on a Bruker AV400 spectrometer operating at 400.13 MHz for proton and 100.61 MHz for carbon.

MALDI-TOF spectra were acquired on an Autoflex apparatus from Bruker Daltonics, equipped with a nitrogen laser (337 nm) and the Flex Control software. The positive reflectron mode was used, with an ion source 1 of 19.00 kV, an ion source 2 of 16.40 kV, a lens of 8.60 kV, a reflector of 20.00 kV, a pulsed ion extraction of 60 ns, a laser frequency of 5.0 Hz (20 shots) and a laser attenuation between 40 and 50%. Solutions of the mixtures of analyte/matrix/salt were prepared in THF and drop cast directly on the substrate. For calibration, the peptide calibration standard from Bruker Daltonics was used.

Size exclusion chromatography (SEC) was performed on a Breeze system from Waters equipped with a 717 plus autosampler, a 1525 Binary HPLC pump, and a 2410 refractive index detector. Three Styragel columns HR3, HR4, and HR6 (all three 7.8 × 300 mm, packed with 5 μm polystyrene-divinylbenzene particles, with pore sizes of 10^3, 10^4, and 10^6 Å, respectively, for effective molecular weight ranges of $500-3\times10^4$, $5\times10^3-6\times10^5$, and $2\times10^5-1\times10^7$, respectively) in series (from Waters) were used for resolution of the different samples. The flow rate of the eluent (THF) was 1 mL/min. The temperature of the columns was 33 °C. Calibration was performed using the polystyrene kit SM-105 (10 points) from Shodex.

Light scattering (LS) experiments (Dawn in 60 s) for the determination of M_w of polymers **1d** and **4b** were performed on a Dawn Eos multiangle light scattering detector (with a wavelength of 690 nm and a laser power of 20 mW) coupled with an Optilab rex refractive index detector, both from Wyatt Technology Corporation. For both samples, dn/dc was determined online assuming total mass recovery. The solvent was chloroform, the pump was a Waters 510 and the autosampler an AS-2000A from Hitachi. The control of the instrument and analysis of data were carried out with Astra 5.1.9.1 of Wyatt.

Preparation of polymer films for mechanical tests was carried out by evaporating a concentrated DCM solution (100 mg/mL) of the desired polymer in a PTFE mold (2 × 2 cm) under atmospheric pressure for 24 h and then under reduced pressure for another 24 h. Smaller rectangular samples (3.5 mm × 2 cm) were cut from these films and used for mechanical tests (dimensions of the films were measured with an electronic digital caliper with a precision of 0.01 mm). Dynamic mechanical analysis was carried out on a DMA 2980 dynamic mechanical analyzer from TA Instruments. For multifrequency experiments, a preload force of 0.02 N, an amplitude of 10 μm, a temperature sweeping rate of 1 °C/min and frequencies of 1, 10, and 100 Hz were used. T_gs determined by DMA were defined as the inflection point in the change of storage modulus. For controlled force (stress−strain) experiments, a preload force of 0.02 N and a force ramp of 0.5 N/min were used. For shape-memory experiments, the controlled force mode was used. In a typical conventional experiment, the sample was stretched to at least 200%, at 1 N/min, after equilibration for 1 min at a temperature 10 °C above the T_g (T_g + 10) of the polymer (determined by multifrequency experiment at 1 Hz). The suitable final static force was estimated from controlled force experiments at the same temperature. The DMA chamber was then cooled down to 10 °C lower than the T_g (T_g − 10) of the polymer and equilibrated for 5 min. The stress was then released (to a preload force of 0.01 N) and the sample allowed to relax at T_g − 10 for 5 min. The temperature was finally raised back up to T_g + 10 at 10 °C/min and the sample allowed to relax at this temperature for 5 min. In a typical cold drawing experiment, the sample was stretched to at least 150%, at 1 N/min, after equilibration for 5 min at T_g − 10. The suitable final static force was estimated from controlled force experiments at the same temperature. The sample was kept under the same static force for further 5 min at T_g − 10 before the stress was released (to a preload force of 0.01 N) and the sample allowed to relax at T_g − 10 for 5 min. The temperature was finally raised back up to T_g + 10 at 10 °C/min and the sample was allowed to relax at this temperature for 5 min. At least three consecutive cycles were performed for each sample and experiments were carried out in quintuplet.

Preparation of the Materials. *Diene **6a***. Please refer to Schemes 1−3 for the details of the titles used for each compound. *N*-2'-Hydroxyethyl-3α-hydroxy-5β-cholan-24-amide (**5a**; 10.0 g, 23.8 mmol), DCM (anhydrous, 200 mL), and triethylamine (freshly distilled, 10.0 mL, 71.7 mmol) were placed in a flame-dried round-bottom flask (three-neck, 500 mL) fitted with a pressure equalizing dropping funnel, under nitrogen. The mixture was cooled down to 0 °C and freshly distilled ω-undecenoyl chloride (14.4 g, 71.4 mmol) was added via the dropping funnel over 1 h. Compound **5a** slowly dissolved and a precipitate (triethylamonium chloride salt) formed. The resulting mixture was stirred overnight at room temperature and poured into dilute aqueous hydrochloric acid (0.1 M, 500 mL). The organic phase was then extracted with water (3 × 250 mL), dried with magnesium sulfate, and filtered and the solvent was evaporated off. Chromatography (silica gel, petroleum ether/ethyl acetate 40/60) afforded the desired compound as a colorless oil (14.3 g, 83%). IR (NaCl, cm^{-1}) 3296, 3076, 2928, 2855, 1736 (C═O), 1679 (sh), 1648, 1545, 1465, 1452, 1419, 1380, 1357, 1328, 1240, 1173, 1118, 992, and 909; ^{1}H NMR ($CDCl_3$, ppm) δ 5.81 (2H; m; C<u>H</u>═C), 5.72 (1H, t, J = 5.1 Hz; N<u>H</u>), 5.03−4.88 (4H, m, C<u>H$_2$</u>═C), 4.72 (1H, m, H-3), 4.17 (2H, t, J = 5.3 Hz, C<u>H$_2$</u>OCO), 3.51 (2H, q, J = 5.4 Hz; C<u>H$_2$</u>NHCO), 2.37−0.81 (66H, mm), and 0.64 (3H, s, 18-C<u>H$_3$</u>); ^{13}C NMR ($CDCl_3$, ppm) δ 12.50, 18.82, 21.28, 23.78, 24.63, 25.36, 25.52, 26.77, 27.15, 27.47, 28.70, 29.33, 29.49, 29.51, 29.54, 29.58, 29.64, 29.67, 29.73, 29.75, 32.16, 32.75, 34.05, 34.22, 34.23, 34.63, 35.05, 35.23, 35.50, 35.95, 36.24, 39.32, 40.61, 40.86, 42.36, 43.20, 56.52, 56.94, 63.57, 74.52, 114.59 (C═C), 114.64 (C═C), 139.57 (C═C), 139.63 (C═C), 173.89 (C═O), 174.11 (C═O), and 174.45 (C═O); (47 obs, 48 req); MS (MALDI-TOF) observed for $C_{48}H_{81}O_5NNa^+$, 774.5; calcd, 774.6; Elem. anal. (carried out on an EAS 1108 instrument from Fisons Instruments): Calcd.: C, 76.6%; H, 10.9%; N, 1.9%. Found: C, 76.4%; H, 10.5%; N, 1.9%.

*Diene **6b***. This compound was prepared, following a similar procedure as for diene **6a**, from *N*-2′-aminoethyl-3α-hydroxy-5β-cholan-24-amide (**5b**; 9.50 g, 22.7 mmol), DCM (anhydrous, 300 mL), triethylamine (freshly distilled, 9.7 mL, 70 mmol), and

Scheme 1. Macrocycles 2a−c are in Equilibrium with their Corresponding Polymers

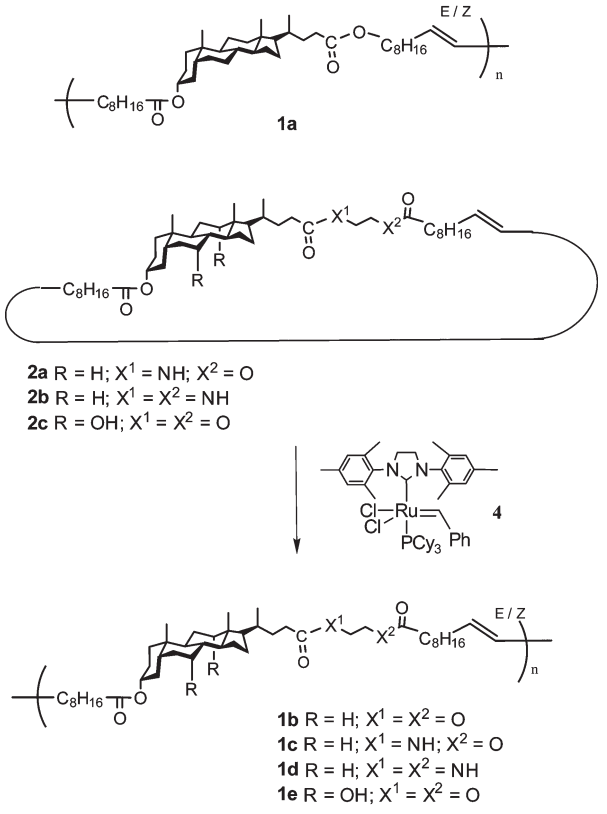

Scheme 2. Synthesis of Macrocycles 2a−c

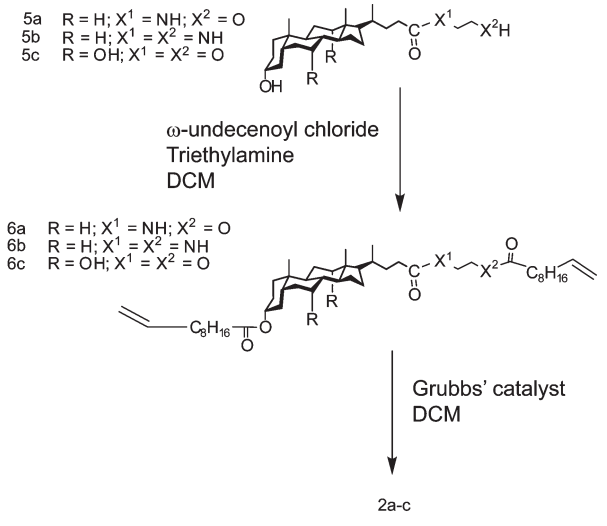

freshly distilled ω-undecenoyl chloride (13.7 g, 68.0 mmol). Chromatography (silica gel, ethyl acetate/methanol 95/5) afforded the desired product as a colorless oil (13.7 g, 81%). IR (NaCl, cm^{-1}) 3295, 3213 (sh), 3080, 2973 (sh), 2927, 2855, 1736 (C═O), 1639, 1555, 1466, 1449, 1422 (sh), 1380, 1243, 1174, 1118, 992, and 909; ^{1}H NMR ($CDCl_3$, ppm) δ 6.45 (2H, s, NH), 5.79 (2H, m, CH═C), 5.01−4.87 (4H, m, CH_2═C), 4.71 (1H, m, H-3), 3.35 (4H, t, J = 2.3 Hz, CH_2NHCO), 2.28−0.95 (60H, mm), 0.91 (3H, s, 19-CH_3), 0.90 (3H, d, J = 8 Hz, 21-CH_3), and 0.62 (3H, s, 18-CH_3); ^{13}C NMR ($CDCl_3$, ppm) δ 12.37, 18.71, 21.15, 23.65, 24.51, 25.38, 26.11, 27.00, 27.34, 28.58, 29.19, 29.22, 29.35, 29.40, 29.44, 29.50, 29.59, 29.67, 29.70, 29.71, 32.17, 32.61, 33.83, 34.09, 34.10, 34.90, 35.07, 35.36, 35.89,

Scheme 3. Synthesis of Copolymers 4a−c

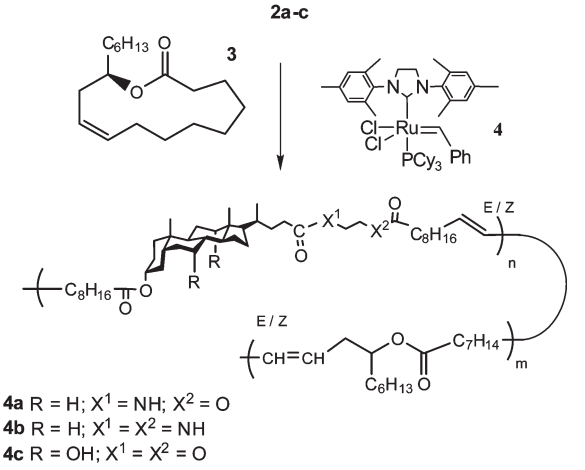

36.10, 36.93, 40.22, 40.28, 40.47, 40.72, 42.21, 43.04, 56.39, 56.78, 74.38, 114.47 (C═C), 114.51 (C═C), 139.35 (C═C), 139.42 (C═C), 173.74 (C═O), 174.93 (C═O) and 175.37 (C═O); (47 obs, 48 req); MS (MALDI-TOF) observed for $C_{48}H_{82}O_4N_2Na^+$, 773.5; calcd, 773.6; Elem. anal. Calcd: C, 76.7%; H, 11.0%; N, 3.7%. Found: C, 76.8%; H, 11.5%; N, 3.7%.

*Diene **6c***. This compound was prepared, following a similar procedure as for diene **6a**, from ethyleneglycol cholate (**5c**) (12.0 g, 26.5 mmol), DCM (anhydrous, 200 mL), triethylamine (freshly distilled, 8.80 mL, 64.1 mmol), and freshly distilled ω-undecenoyl chloride (11.8 g, 58.3 mmol). Chromatography (silica gel, petroleum ether/ethyl acetate 80/20) and recrystallization from ethyl acetate and hexane afforded a white powder (13.3 g, 64%). T_m (DSC) 88 °C; IR (NaCl, cm^{-1}) 3492, 3076, 2969 (sh), 2928, 2856, 1738 (C═O), 1641, 1464, 1447, 1418, 1379, 1360, 1243, 1171, 1096, 1073, 1040, 994, and 911; ^{1}H NMR ($CDCl_3$, ppm) δ 5.80 (2H, m, CH═C), 5.02−4.89 (4H, m, CH_2═C), 4.57 (1H, m, H-3), 4.26 (4H, s, CH_2OCO), 3.98 (1H, m, H-12), 3.85 (1H, m, H-7), 2.44−1.00 (56H, mm), 0.98 (3H, d, J = 6.2 Hz, 21-CH_3), 0.90 (3H, s, 19-CH_3), and 0.69 (3H, s, 18-CH_3); ^{13}C NMR ($CDCl_3$, ppm) δ 12.99, 17.76, 22.97, 23.57, 25.30, 25.48, 27.14, 27.16, 27.86, 28.83, 29.32, 29.50, 29.53, 29.57, 29.64, 29.72, 29.73, 31.19, 31.48, 34.21, 34.23, 34.56, 34.83, 35.12, 35.23, 35.32, 35.54, 35.67, 39.99, 41.63, 42.50, 46.98, 47.62, 62.44, 62.51, 68.68, 73.32, 74.42, 114.55 (C═C), 114.60 (C═C), 139.59 (C═C), 139.66 (C═C), 173.97 (C═O), 174.04 (C═O), and 174.39 (C═O); (45 obs, 48 req); MS (MALDI-TOF) observed for $C_{48}H_{80}O_8Na^+$, 807.4; calcd, 807.6; Elem. anal. Calcd: C, 73.4%; H, 10.3%. Found: C, 73.5%; H, 9.0%.

*Cyclic Bile Acid **2a***. Diene **6a** (10.0 g, 13.3 mmol) and DCM (anhydrous, 1.5 L) were placed in a flame-dried round-bottom flask (two-neck, 2 L), under an argon atmosphere. The resulting mixture was degassed with argon for 2 h and a solution of benzylidene-bis(tricyclohexylphosphine) dichlororuthenium (Grubbs' catalyst first generation; 547 mg, $6.65.10^{-4}$ mol) in DCM (anhydrous, argon degassed, 50 mL) was added. Stirring at room temperature was continued for 24 h and ethylvinyl ether (5 mL, excess) was added to quench the catalyst. After stirring for a further 3 h, the solvent was evaporated off and the resulting dark brown oil was purified by chromatography (silica gel, petroleum ether/ethyl acetate 50/50) to afford the desired compound as a colorless solid (6.47 g, 67%). T_m (DSC) 13 °C; IR (NaCl, cm^{-1}) 3300, 3075, 2927, 2855, 1735 (C═O), 1675 (sh), 1649, 1546, 1460 (sh), 1450, 1380, 1241, 1174, 1121, and 966; ^{1}H NMR ($CDCl_3$, ppm) δ 5.77 (1H, t, J = 5.1 Hz, NH), 5.43−5.29 (2H, mm, CH═), 4.74 (1H, m, H-3), 4.18 (2H, t, J = 4.9 Hz; CH_2OCO), 3.52 (2H, m, CH_2NHCO), 2.36−0.97 (60H, mm), 0.93 (3H, d, J = 5.9 Hz; 21-CH_3), 0.92 (3H, s, 19-CH_3), and 0.64 (3H, s, 18-CH_3); ^{13}C NMR ($CDCl_3$, ppm) δ 12.44, 18.84, 21.28, 23.75, 24.60, 25.35,

25.55, 26.75, 27.09, 27.41, 28.68, 29.00, 29.05, 29.35, 29.52, 29.55, 29.57, 29.69, 29.72, 29.82, 30.02, 32.27, 32.69, 32.86, 33.00, 33.54, 34.66, 34.99, 35.33, 35.45, 35.73, 36.18, 39.47, 40.64, 40.89, 42.27, 43.16, 56.04, 57.04, 63.54, 74.41, 130.69 (C=C), 130.79 (C=C), 173.90 (C=O), 174.16 (C=O), and 174.53 (C=O); (46 obs, 46 req); MS (MALDI-TOF) observed for $C_{46}H_{77}O_5NNa^+$, 746.4 g·mol^{-1}; calcd, 746.6 g·mol^{-1}; Elem. anal. Calcd: C, 76.3%; H, 10.7%; N, 1.9%. Found: C, 76.0%; H, 9.9%; N, 1.9%.

Cyclic Bile Acid ***2b***. The title compound was prepared, following a similar procedure as for cyclic bile acid **2a**, from diene **6b** (2.00 g, 2.66 mmol), benzylidene-bis(tricyclohexylphosphine) dichlororuthenium (Grubbs' catalyst first generation; 110 mg, 1.33.10^{-4} mol), and DCM (anhydrous, 200 mL). Chromatography (silica gel, ethyl acetate/methanol 95/5) afforded the desired compound as a colorless solid (1.09 g, 57%). T_m (DSC) 134 °C; IR (NaCl, cm^{-1}) 3299, 3220 (sh), 3080, 2971, 2927, 2854, 1731 (C=O), 1670 (sh), 1649, 1546, 1464, 1449, 1378, 1334, 1246, 1176, 1020, and 966; ^{1}H NMR ($CDCl_3$, ppm) δ 6.34 (2H, s, NH), 5.43−5.29 (2H, mm, CH=), 4.74 (1H, m, H-3), 3.48−3.29 (4H, m, CH_2NHCO), 2.31−0.97 (60H, mm), 0.92 (3H, s, 19-CH_3), 0.91 (3H, d, J = 6.4 Hz, 21-CH_3), and 0.64 (3H, s, 18-CH_3); ^{13}C NMR ($CDCl_3$, ppm) δ 12.45, 18.81, 21.29, 23.75, 24.61, 25.55, 26.14, 26.74, 27.08, 27.42, 28.76, 28.99, 29.00, 29.30, 29.60, 29.70, 29.72, 29.75, 29.76, 29.82, 30.05, 32.35, 32.69, 32.85, 33.03, 33.89, 34.99, 35.33, 35.45, 36.11, 36.19, 37.15, 40.62, 40.76, 40.88, 42.27, 43.17, 56.30, 56.99, 74.41, 130.65 (C=C), 130.81 (C=C), 173.95 (C=O), 175.20 (C=O), and 175.66 (C=O); (45 obs, 46 req); MS (MALDI-TOF) observed for $C_{46}H_{78}O_4N_2Na^+$, 745.5; calcd, 745.6; Elem. anal. Calcd: C, 76.4%; H, 10.9%; N, 3.9%. Found: C, 75.4%; H, 11.2%; N, 3.7%.

Cyclic Bile Acid ***2c***. The title compound was prepared, following a similar procedure as for cyclic bile acid **2a**, from diene **6c** (2.00 g, 2.55 mmol), benzylidene-bis(tricyclohexylphosphine) dichlororuthenium (Grubbs' catalyst first generation; 105 mg, 1.27.10^{-4} mol), and DCM (anhydrous, 200 mL). Chromatography (silica gel, petroleum ether/ethyl acetate 75/25) and recrystallization in ethyl acetate/hexane afforded the desired compound as a colorless solid (1.02 g, 53%). T_m (DSC) 119 °C; IR (NaCl, cm^{-1}) 3452, 3385, 2974, 2925, 2854, 1738 (C=O), 1462, 1377, 1301, 1253, 1173, 1075, 1039, and 966; ^{1}H NMR ($CDCl_3$, ppm) δ 5.44−5.29 (2H, mm, CH=), 4.59 (1H, m, H-3), 4.35−4.18 (4H, m, CH_2OCO), 3.97 (1H, m, H-12), 3.85 (1H, m, H-7), 2.42−1.03 (56H, mm), 1.00 (3H, d, J = 10.2 Hz, 21-CH_3), 0.90 (3H, s, 19-CH_3), and 0.70 (3H, s, 18-CH_3); ^{13}C NMR ($CDCl_3$, ppm) δ 12.96, 17.78, 23.00, 23.53, 25.31, 25.55, 27.08, 27.32, 27.79, 29.00, 29.12, 29.14, 29.19, 29.43, 29.56, 29.59, 29.71, 29.77, 30.07, 30.85, 31.25, 32.91, 33.05, 34.65, 34.82, 35.04, 35.22, 35.27, 35.44, 35.62, 39.98, 41.60, 42.71, 46.78, 46.90, 62.59, 62.55, 68.58, 73.22, 74.32, 130.75 (C=C), 130.84 (C=C), 174.02 (C=O), 174.10 (C=O), and 174.51 (C=O); (45 obs, 46 req); MS (MALDI-TOF) observed for $C_{46}H_{76}O_8Na^+$, 779.4; calcd, 779.5; Elem. anal. Calcd: C, 73.0%; H, 10.1%. Found: C, 72.8%; H, 9.2%.

ED-ROMP General Procedure. *Polymer* ***1c***. Cyclic bile acid **2a** (290 mg, 4.01 × 10^{-4} mol) and DCM (anhydrous, degassed with argon for 1 h, 250 μL) were placed in a flame-dried round-bottomed flask (1-neck, 10 mL) under argon. A solution of 1,3-bis-(2,4,6-trimethylphenyl)-2-imidazolidinylidene)dichloro(phenylmethylene)-(tricyclohexylphosphine)ruthenium; Grubbs' catalyst second generation in DCM (83 μL of a solution of 10.2 mg, 1.20 × 10^{-5} mol, in 250 μL degassed anhydrous DCM, amounting to 1 mol % with respect to the monomer) was added via a septum. The mixture was left to react at room temperature for 30 min. The vigorously stirred solution rapidly became very viscous and eventually stirring stopped. Ethyl vinyl ether (0.1 mL) was added and left to diffuse for 1 h to quench the catalyst and DCM (10 mL) was added. The resulting viscous solution was precipitated in a hexane/methanol 2/1 mixture (200 mL). The colorless gum that precipitated was filtered off, quickly dried in vacuum, dissolved in DCM (10 mL), and precipitated in a hexane/methanol 2/1 mixture (200 mL). Filtration and drying in vacuum for one day afforded a colorless gum (274 mg, 94%). DSC: T_g, 44 °C; TGA: T_{dec}, 350 °C; IR (NaCl, cm^{-1}) 3433 (sh), 3366 (sh), 3300, 3222 (sh), 3075, 2927, 2854, 1733 (C=O), 1679 (sh), 1651, 1547, 1464, 1454, 1422, 1380, 1239, 1175, 1120, 990, and 967; ^{1}H NMR ($CDCl_3$, ppm) δ 5.81 (1H, m, NH), 5.42−5.29 (2H, mm, CH=), 4.72 (1H, m, H-3), 4.15 (2H, t, J = 5.3 Hz, CH_2OCO), 3.51 (2H, q, J = 5.5 Hz, CH_2NHCO), 2.34−0.81 (66H, mm), and 0.63 (3H, s, 18-CH_3); ^{13}C NMR ($CDCl_3$, ppm) δ 12.49, 18.82, 21.28, 23.78, 24.63, 25.36, 25.52, 25.71, 26.77, 27.14, 27.47, 27.64, 28.69, 29.54, 29.57, 29.68, 29.70, 29.76, 29.78, 30.06, 32.14, 32.75, 34.05, 34.62, 35.04, 35.21, 35.50, 35.96, 36.24, 39.26, 40.60, 40.85, 42.35, 43.19, 56.55, 56.92, 63.54, 74.52, 130.72 (C=C), 130.75 (C=C), 130.76 (C=C), 130.80 (C=C), 173.88 (C=O), 174.11 (C=O), and 174.42 (C=O); (45 obs, 46 req); SEC (THF) M_n 223900; M_w 397000; Elem. anal. Calcd for $(C_{46}H_{77}O_5N)_n$: C, 76.3%; H, 10.7%; N, 1.9%. Found: C, 75.8%; H, 11.2%; N, 1.9%.

Polymer ***1d***. The title polymer was prepared, following a similar procedure as for polymer **1c**, from cyclic bile acid **2b** (250 mg, 3.46.10^{-4} mol), DCM (anhydrous, degassed with argon for one hour, 250 μL), and a solution of 1,3-bis-(2,4,6-trimethylphenyl)-2-imidazolidinylidene)dichloro(phenyl methylene)-(tricyclohexylphosphine)ruthenium; Grubbs' catalyst second generation in DCM (54 μL of a solution of 12.5 mg, 1.47.10^{-5} mol, in 250 μL degassed anhydrous DCM, amounting to 1 mol % with respect to the monomer). This afforded a colorless gum (229 mg, 92%). DSC: T_g, 83 °C; TGA: T_{dec}, 350 °C; IR (NaCl, cm^{-1}) 3290, 3216 (sh), 3083, 2926, 2854, 2696, 1732 (C=O), 1644, 1560 (sh), 1550, 1465, 1449, 1379, 1359, 1245, 1177, 1120, 967, and 912; ^{1}H NMR ($CDCl_3$, ppm) δ 6.68 (2H, bs, NH), 5.43−5.28 (2H, mm, CH=), 4.72 (1H, m, H-3), 3.36 (4H, bs, CH_2NHCO), 2.33−0.81 (66H, mm), and 0.63 (3H, s, 18-CH_3); ^{13}C NMR ($CDCl_3$, ppm) δ 12.52, 18.85, 21.28, 23.79, 24.64, 25.53, 26.24, 26.29, 26.79, 27.14, 27.48, 28.71, 29.41, 29.49, 29.53, 29.57, 29.62, 29.67, 29.72, 29.76, 29.80, 29.86, 30.02, 30.05, 30.09, 32.27, 32.75, 33.03, 35.04, 35.23, 35.50, 36.24, 37.11, 40.60, 40.86, 42.34, 43.19, 56.51, 56.92, 74.52, 130.74 (C=C), 130.77 (C=C), 130.84 (C=C), 173.92 (C=O), 175.11 (C=O), and 175.51 (C=O); (46 obs, 46 req); LS ($CHCl_3$) M_w 400500 ± 23200; Elem. anal. Calcd for $(C_{46}H_{78}O_4N_2)_n$: C, 76.4%; H, 10.9%; N, 3.9%. Found: C, 74.9%; H, 10.0%; N, 3.8%.

Polymer ***1e***. The title polymer was prepared, following a similar procedure as for polymer **1c**, from cyclic bile acid **2c** (250 mg, 3.30.10^{-4} mol), DCM (anhydrous, degassed with argon for 1 h, 250 μL), and a solution of 1,3-bis-(2,4,6-trimethylphenyl)-2-imidazolidinylidene)dichloro(phenyl methylene)-(tricyclohexylphosphine)ruthenium; Grubbs' catalyst second generation in DCM (42 μL of a solution of 16.5 mg, 1.94 × 10^{-5} mol, in 250 μL degassed anhydrous DCM, amounting to 1 mol % with respect to the monomer). This afforded a colorless gum (237 mg, 95%). DSC: T_g, 42 °C; TGA: T_{dec}, 349 °C; IR (NaCl, cm^{-1}) 4508, 2926, 2855, 1732 (C=O), 1464, 1418, 1380, 1251, 1172, 1096, 1074, 969, and 914; ^{1}H NMR ($CDCl_3$, ppm) δ 5.43−5.27 (2H, mm, CH=), 4.57 (1H, m, H-3), 4.26 (4H, s, CH_2OCO), 3.98 (1H, m, H-12), 3.85 (1H, m, H-7), 2.45−0.80 (62H, mm), and 0.69 (3H, s, 18-CH_3); ^{13}C NMR ($CDCl_3$, ppm) δ 12.97, 14.55, 17.77, 22.93, 23.09, 23.62, 25.31, 25.50, 27.06, 27.18, 27.64, 27.91, 28.75, 29.54, 29.62, 29.68, 29.70, 29.76, 30.05, 31.18, 31.51, 31.53, 32.02, 33.03, 34.56, 34.58, 35.14, 35.25, 35.26, 35.64, 39.92, 41.66, 42.44, 46.99, 47.66, 62.44, 62.52, 68.73, 74.47, 130.73 (C=C), 130.76 (C=C), 130.78 (C=C), 130.81 (C=C), 173.98 (C=O), 174.07 (C=O), and 174.44 (C=O); (46 obs, 46 req); SEC (THF) M_n 172300; M_w 319200; Elem. anal. Calcd for $(C_{46}H_{76}O_8)_n$: C, 73.0%; H, 10.1%. Found: C, 72.7%; H, 10.6%.

ED-ROMP Copolymerizations. Copolymers **4a**−**c** were prepared following a similar procedure as for polymer **1c** from the

Table 1. Mechanical and Shape Memory Performance of Bile Acid-Based Polyesters (BAPs)

				shape memory warm drawing (%)		shape memory cold drawing (%)	
	M_w[a] ($\times 10^3$)	T_{gDMA} (°C)	E (MPa)[c] at 37.5 °C	R_r (2)[d]	R_f (2)[d]	R_r (2)[d]	R_f (2)[d]
1a	278	21.0 ± 0.7	2.1 ± 0.3	99.1 ± 0.5	97.9 ± 0.2	99.5 ± 0.5	78.9 ± 1.2
1b	452	13.5 ± 0.4	1.2 ± 0.1	99.7 ± 0.4	98.2 ± 0.1	99.2 ± 0.2	79.9 ± 2.3
1c	397	51.0 ± 2.1	269 ± 97	98.9 ± 0.7	98.1 ± 0.2	97.6 ± 1.3	72.9 ± 2.7
1d[d]	400[b]	63.2 ± 2.9	590 ± 98	96.2 ± 2.3	95.6 ± 0.5	98.6 ± 0.9	76.5 ± 2.8
1e	320	48.8 ± 1.4	406 ± 88	98.7 ± 0.7	94.2 ± 1.8	99.0 ± 0.6	56.1 ± 3.8
4a	415	36.9 ± 0.6	5.83 ± 1.0	99.5 ± 0.2	94.4 ± 1.6	96.3 ± 0.9	68.0 ± 2.5
4b	405[b]	41.6 ± 3.3	75 ± 30	94.6 ± 0.4	90.7 ± 1.8	95.8 ± 1.3	60.7 ± 1.1
4c	270	35.6 ± 0.5	19.6 ± 4.2	99.0 ± 0.7	91.4 ± 2.0	98.2 ± 0.9	65.5 ± 3.9

[a] M_w determined by SEC. [b] M_w determined by light scattering. [c] Young's moduli measured from stress−strain curves. [d] Second shape memory cycle (for the first and third cycles, see Table S1 in the Supporting Information).

corresponding cyclic bile acid (respectively, 81, 63, and 84 mol %) and ricinoleides **3**. The molar ratios of macrocyclic bile acid to ricinoleide were determined from eq 1,[26] using the value of T_g of the respective bile acid-based homopolymers determined by DMA and the extrapolated T_g of the ricinoleide homopolymer (−54.9 °C) as determined in ref 23. Spectroscopic results are consistent with the structures of both monomers, as reported in the present article and the literature.[21,25] Mechanical properties and shape memory performance results are gathered in Table S1.

$$x = \frac{37.5 - T_{g2}}{T_{g1} - T_{g2}} \quad (1)$$

where x is the mole fraction of macrocyclic bile acid required to prepare a copolymer displaying a T_g of 37.5 °C; T_{g1} is the T_g of the bile acid-based homopolymer; and T_{g2} is the T_g of ricinoleide homopolymer.

Results and Discussion

One of the aims of the present article is to demonstrate that the versatility of metathesis chemistry allows the preparation of a wide range of macromolecular architectures. We show that high molecular weight cholic acid-based BAPs, which may be anticipated to be more biocompatible owing to the better tolerance of cholic acid in vivo,[27] can be prepared following our procedure (Scheme 1). In addition, we introduce amide bonds in the polymer backbone to increase its rigidity, glass transition temperature, and Young's modulus. Macrocycles **2a**−**c** were synthesized in relatively high yields (53−67%) using classical high dilution conditions (Scheme 2).[21] ED-ROMP of compounds **2a**−**c** using the second-generation Grubbs' catalyst then afforded high molecular weight polymers **1c**−**e** with high conversions (Table 1).

BAPs **1a**−**e** display T_gs ranging from 13 to 63 °C (Table 1, Figure 1). In the lithocholic acid series, the introduction of more rigid (and potentially hydrogen-bonded) amide bonds induces an increase of T_g (**1b** < **1c** < **1d**). Similarly, the presence of hydroxyl groups in **1e** leads to increased intramolecular interactions and higher thermal energies required for long-range coherent molecular motion, shifting T_gs by about 35 °C. Small changes in the polymer structure provide a simple tool for the tuning of the materials stiffness, which is particularly relevant to the field of soft tissue engineering, given the importance of materials compliance on cell behavior.[28,29] Stress−strain experiments revealed that, above their T_gs, **1a**−**e** behave as typical elastomers with maximal elongations greater than 350−400% (beyond the stretching limit of our instrument geometry, Table 1).

As no covalent cross-links are generated (which is evidenced by the full relaxation of the materials in stress relaxation experiments[21]) and no indication of physical cross-linking (e.g., hydrogen bonds or crystallization) was observed from DSC and preliminary WAXS experiments (results not shown), we hypothesize that entanglement alone is responsible for the elastomeric

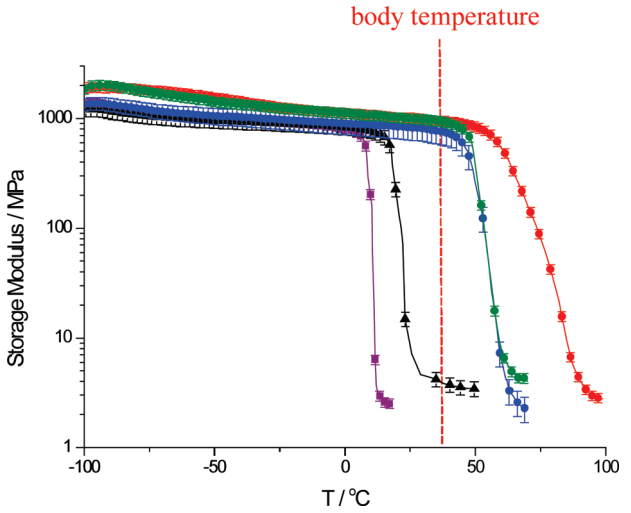

Figure 1. Evolution of the storage modulus of polymers **1a**−**e** with temperature followed by DMA at a frequency of 1 Hz. Measurements were made on rectangular samples (3.5 mm × 2 cm), with a preload force of 0.02 N, an amplitude of 10 μm, and a temperature sweeping rate of 1 °C/min. Black triangles, **1a**; purple squares, **1b**; blue circles, **1c**; red circles, **1d**; green circles, **1e**.

behavior of polymers **1a**−**e**. Examples of non-cross-linked elastomers (comprising only one block) can be found in the family of polyrotaxanes and polycatenanes, in which polymer chains are trapped in dangling cyclic structures or loops.[30−32] In addition, entanglement plays a role in the rheological behavior of gels and the elasticity of polymer networks.[33−36] Entanglement and non-permanent topological "cross-links" may have a similar effect to chemical cross-links on elasticity, at least at intermediate time and physical scales.[35−37] Therefore, it is possible that chain entanglement and the formation of kinetic topological "cross-links" give rise to macroscopic elastic behaviors on a sufficiently long time scale in bile acid-based shape memory polymers **1a**−**e**. There are no loops dangling from the polymeric backbone in these materials, but it is not clear whether a small portion of free cyclic polymers contributes to the elastic behavior nor to what extent.[38] Below T_g, although **1a**−**e** are relatively brittle, with high Young's moduli, if slowly stretched they display high ultimate strains at break (beyond the 400% capacity of our geometry). This phenomenon is believed to be due to a lower T_g when stretched at a slow rate, consistent with the normal behavior of visco-elastic materials and the Williams−Landel−Ferry equation.[39] Multi-frequency experiments reveal that T_gs of polymers **1a**−**e** are lowered by about 4.1 ± 0.4 °C upon decreasing the frequency by a factor of 10. This phenomenon allows the use of BAPs as SMPs in the cold drawing mode, thus, simplifying programming procedures.

Polymers **1a**−**e** are high performance SMPs in both warm and cold drawing mode. In the warm drawing mode (Figure 2), the sample is

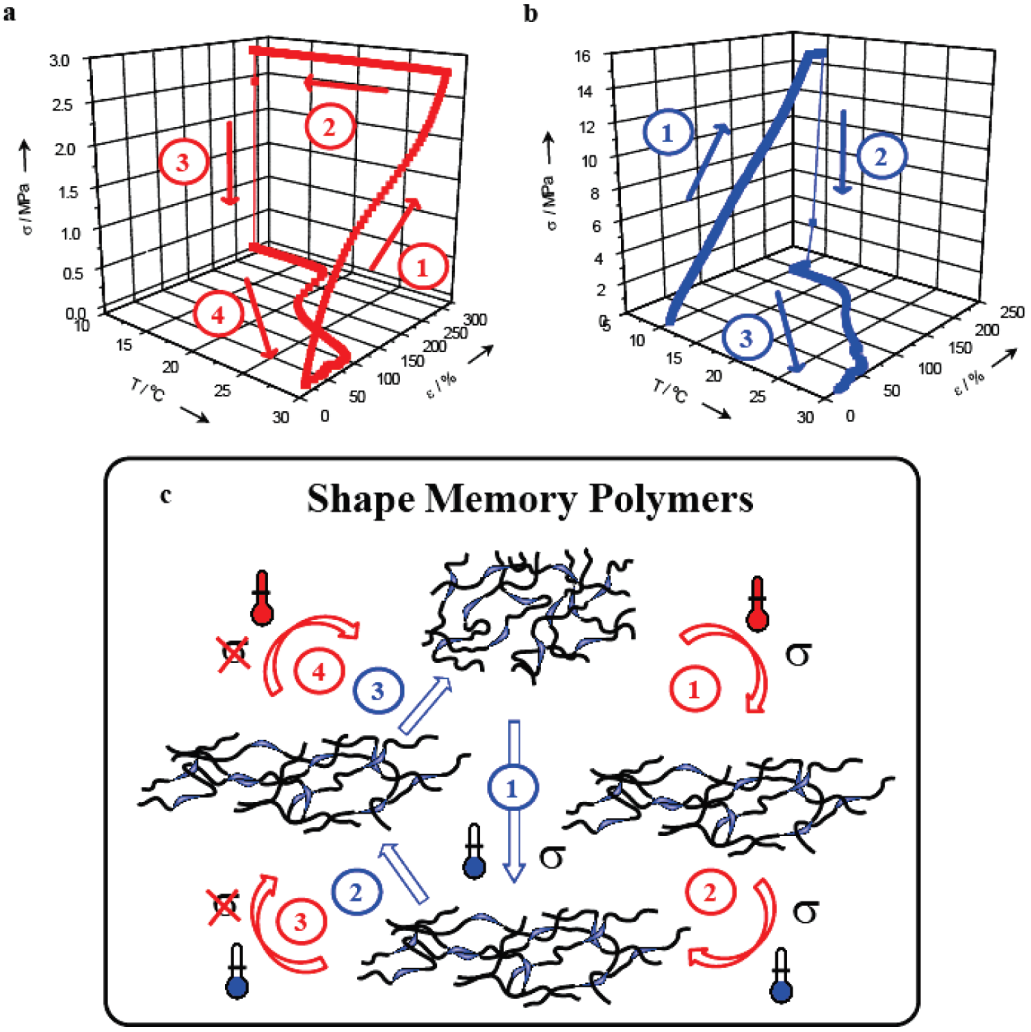

Figure 2. Shape memory phenomenon in bile acid-based polyesters. (a) Typical warm drawing experiment: the sample is warmed above its transition temperature (1), stretched/deformed to the desired temporary shape (2), the temperature is dropped to fix the temporary shape (3), and shape recovery is triggered by warming the sample above its transition temperature (4). (b) Cold drawing experiment: the sample is directly stretched below its transition temperature (1) and the remaining steps are as for the warm drawing. (c) Shape memory effect in warm (red) and cold (blue) drawing mode. The cold drawing cycle is shorter, which simplifies its use and application in devices. The numbers in red and blue correspond to the thermomechanical steps depicted in (a) and (b), respectively.

stretched (to 300% strain) above its T_g and then cooled down to $T_g - 10$ before suppressing the applied stress. Some relaxation occurs, which is quantified by the strain fixity R_f (eq 2). Upon warming back up to $T_g + 10$, the permanent shape is recovered, as characterized by the strain recovery R_r (eq 3)

$$R_f(N) = \frac{\varepsilon_u(N)}{\varepsilon_m} \quad (2)$$

$$R_r(N) = \frac{\varepsilon_m - \varepsilon_p(N)}{\varepsilon_m - \varepsilon_p(N-1)} \quad (3)$$

where N is the cycle number, ε_m is the maximum strain, ε_u is the strain after relaxation at $T_g - 10$, and ε_p is the strain after recovery. In the cold drawing mode, the sample is stretched below its T_g (150% strain). Cold drawing shape memory effect is not as often encountered due to the difficulty of stretching most materials below their transition temperature to substantial strains without failure. Figure 3 shows typical examples of shape recovery with BAPs.

The performance of **1a**−**e** in both warm and cold drawing was evaluated for at least three consecutive thermomechanical cycles (Tables 1 and S1). In the warm drawing mode R_fs and R_rs are high (90−98%). Cycling experiments reveal a small training effect due to the occurrence of some chain relaxation during the first mechanical cycle, leading to 1−5% deviation with the second cycle, which is characteristic of SMPs (Figure 4).[7] Subsequent cycles are remarkably superimposable. Strain recoveries measured in the cold drawing mode remained reasonably high (above 93%), but strain fixities decreased to varying extents (80 to 56%). This phenomenon is thought to arise from slower chain relaxations at low stretching temperatures. In the warm drawing mode chain relaxation occurs faster, mostly during sample stretching. This may also explain why little training effect is observed in the cold drawing mode. To further study whether slow relaxation of the deformed samples occurs over extended periods of time, we stretched a sample of polymer **1e** and left it at room temperature (below its T_g) for a period of 1 month. After the initial slight relaxation typical of shape memory materials, the sample did not further relax, however, when heated with warm air it quickly recovered its initial shape (with recoveries typical of those reported in thermomechanical cycling measurements).

To demonstrate the potential of BAPs for application in stent grafts, a tubular sample was folded into a thinner rod. Upon warming, the sample fully recovered its tubular shape in a few

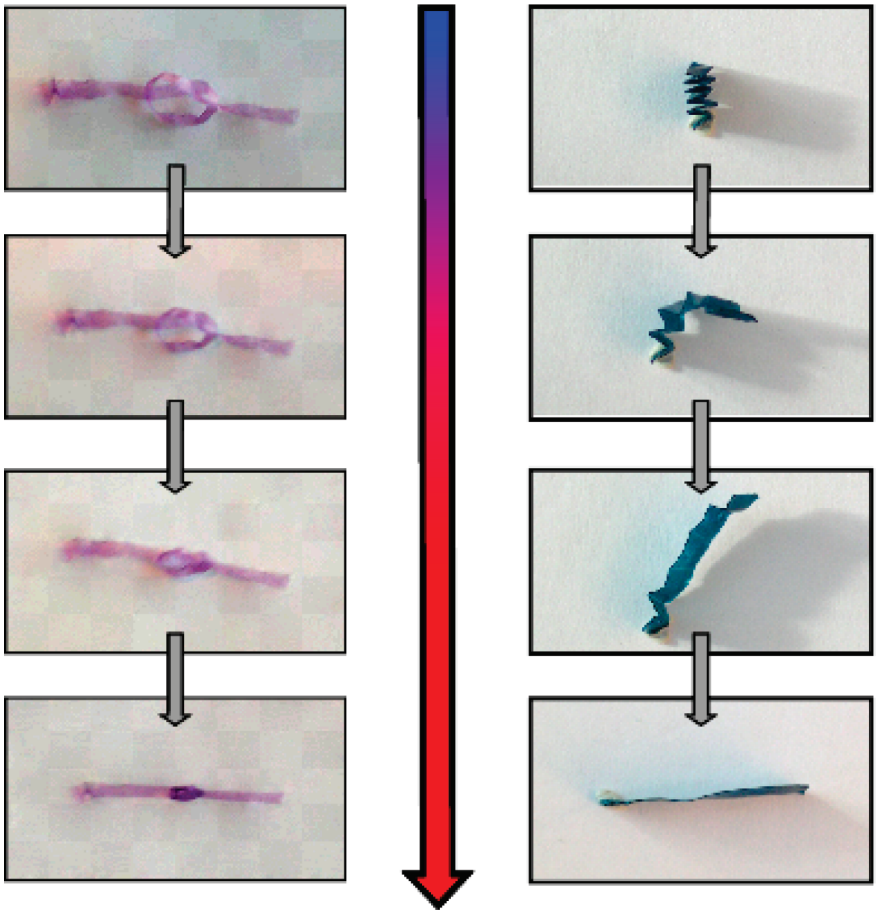

Figure 3. Examples of shape recovery for two samples stained with methylene blue to help their visualization (all bile acid-based polymers prepared being transparent and colorless). Left: a thread of polymer **1a** was stretched to about 200% of its original length below its transition temperature and tied into a loose knot. Warming the sample to room temperature triggers the shape recovery event which results in the tightening of the knot. Right: a sample of polymer **1c** was folded and recovers its shape in a few seconds when gently heated with warm air.

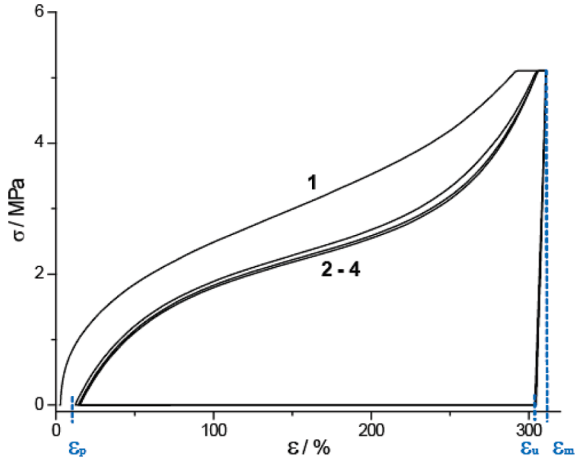

Figure 4. Stress−strain plots recorded for four subsequent thermal cycles (respective cycle numbers indicated on the graph) carried out in warm drawing mode on a sample of polymer **1e**.

seconds. For biomedical applications, triggering shape recovery at high temperature may not be practically feasible, although approaches to tackle this problem have been developed.[40] However, we found that the shape recovery temperature of bile acid-*co*-ricinoleic acid copolyesters (see Scheme 3) can be predicted and tuned with remarkable precision simply by adjusting the molar composition of the copolymer.[23] Macrocycles **2a**−**c** were copolymerized with required amounts of ricinoleides (as predicted by eq 1) to obtain copolymers **4a**−**c** with T_gs at 37.5 °C. As predicted, polymers **4a**−**c** display T_gs near body temperature (see Table 1) while retaining excellent shape memory properties. Slight divergence with predictions may be due to differences in rates of polymerization, as well as deviations from eq 1 (which assumes equal volume−temperature coefficients).[26] Therefore, polymeric scaffolds based on such materials offer a remarkable freedom of design: their chemical structure may be altered (e.g., to improve their biocompatibility, enhance cell adhesion or release specific factors) while maintaining a good control of their shape recovery temperature and mechanical properties. Overall, we have so far shown that BAPs may be tailored to display T_gs and shape recovery over a range of temperatures spanning nearly 100 °C.[23,24]

Conclusion

ED-ROMP is a useful tool for the synthesis of a wide range of novel polymers. If reaction conditions are carefully optimized, the starting cyclic monomers can be prepared in relatively large quantities, viable for biomedical applications. We established that BAPs are a class of degradable materials that show tunable mechanical properties and exceptional shape memory effect useful for the design of biomedical devices such as all-polymeric stent grafts and smart suture materials. The ease with which their chemical structure can be modified and the possibility of copolymerizing with other macromonomers derived from natural origins presents a fantastic opportunity for the design of biomaterials with well controlled mechanical and chemical properties as well as biocompatibility and bioresponsiveness.

Acknowledgment. The authors thank Profs. Peter Cormack and Adi Eisenberg for helpful discussion. Financial support from NSERC of Canada, FQRNT of Quebec, and the Canada Research Chair Program is gratefully acknowledged.

Supporting Information Available: Shape memory performance as determined by thermomechanical cycling. This material is available free of charge via the Internet at http://pubs.acs.org.

References and Notes

(1) Barras, C. D. J.; Myers, K. A. *Eur. J. Vasc. Endovasc. Surg.* **2000**, *19*, 564–569.
(2) Lendlein, A.; Kelch, S. *Angew. Chem., Int. Ed.* **2002**, *41*, 2034–2057.
(3) Miaudet, P.; Derre, A.; Maugey, M.; Zakri, C.; Piccione, P. M.; Inoubli, R.; Poulin, P. *Science* **2007**, *318*, 1294–1296.
(4) Lendlein, A.; Langer, R. *Science* **2002**, *296*, 1673–1676.
(5) Alteheld, A.; Feng, Y.; Kelch, S.; Lendlein, A. *Angew. Chem., Int. Ed.* **2005**, *44*, 1188–1192.
(6) Chung, T.; Rorno-Uribe, A.; Mather, P. T. *Macromolecules* **2008**, *41*, 184–192.
(7) Rabani, G.; Luftmann, H.; Kraft, A. *Polymer* **2006**, *47*, 4251–4260.
(8) Kelch, S.; Steuer, S.; Schmidt, A.; Lendlein, A. *Biomacromolecules* **2007**, *8*, 1018–1027.
(9) Yakacki, C. M.; Shandas, R.; Lanning, C.; Rech, B.; Eckstein, A.; Gall, K. *Biomaterials* **2007**, *28*, 2255–2263.
(10) Chen, M.-C.; Tsai, H.-W.; Chang, Y.; Lai, W.-Y.; Mi, F.-L.; Liu, C.-T.; Wong, H.-S.; Sung, H.-W. *Biomacromolecules* **2007**, *8*, 2774–2780.
(11) Hofmann, A. F.; Roda, A. *J. Lipid Res.* **1984**, *25*, 1477–1489.
(12) Fu, K.; Pack, D. W.; Klibanov, A. M.; Langer, R. *Pharm. Res.* **2000**, *17*, 100–106.
(13) Gautrot, J. E.; Zhu, X. X. *J. Biomater. Sci., Polym. Ed.* **2006**, *17*, 1123–1139.
(14) Janout, V.; Regen, S. L. *J. Am. Chem. Soc.* **2005**, *127*, 22–23.
(15) Hodge, P.; Colquhoun, H. M. *Polym. Adv. Technol.* **2005**, *16*, 84–94.
(16) Kamau, S. D.; Hodge, P.; Helliwell, M. *Polym. Adv. Technol.* **2003**, *14*, 492–501.
(17) Okajima, S.; Kondo, R.; Toshima, K.; Matsumura, S. *Biomacromolecules* **2003**, *4*, 1514–1519.
(18) Hori, Y.; Hongo, H.; Hagiwara, T. *Macromolecules* **1999**, *32*, 3537–3539.
(19) Hodge, P.; Kamau, S. D. *Angew. Chem., Int. Ed.* **2003**, *42*, 2412–2414.
(20) Kamau, S. D.; Hodge, P.; Hall, A. J.; Dad, S.; Ben-Haida, A. *Polymer* **2007**, *48*, 6808–6822.
(21) Gautrot, J. E.; Zhu, X. X. *Angew. Chem., Int. Ed.* **2006**, *45*, 6872–6874.
(22) Gao, W.; Hagver, R.; Shah, V.; Xie, W.; Gross, R. A.; Ilker, M. F.; Bell, C.; Burke, K. A.; Coughlin, E. B. *Macromolecules* **2007**, *40*, 145–147.
(23) Gautrot, J. E.; Zhu, X. X. *Chem. Commun.* **2008**, *14*, 1674–1676.
(24) Gautrot, J. E.; Zhu, X. X. *J. Mater. Chem.* **2009**, *19*, 5705–5716.
(25) Slivniak, R.; Domb, A. J. *Biomacromolecules* **2005**, *6*, 1679–1688.
(26) Wood, L. A. *J. Polym. Sci.* **1958**, *28*, 319–330.
(27) Gauthier, M.; Simard, P.; Zhang, Z.; Zhu, X. X. *J. R. Soc. Interface* **2007**, *4*, 1145–1150.
(28) Collin, O.; Trackqui, P.; Stephanou, A.; Usson, Y.; Clement-Lacroix, J.; Planus, E. *J. Cell Sci.* **2006**, *119*, 1914–1925.
(29) Engler, A. J.; Sen, S.; Sweeney, H. L.; Discher, D. E. *Cell* **2006**, *126*, 677–689.
(30) Okumura, Y.; Ito, K. *Adv. Mater.* **2001**, *13*, 485–487.
(31) Araki, J.; Ito, K. *Soft Matter* **2007**, *3*, 1456–1473.
(32) Muscat, D.; Kohler, W.; Rader, H. J.; Martin, K.; Mullins, S.; Muller, B.; Geerts, Y. *Macromolecules* **1999**, *32*, 1737–1745.
(33) Likhtman, A. E.; Sukumaran, S. K.; Ramirez, J. *Macromolecules* **2007**, *40*, 6748–6757.
(34) Ball, R. C.; Doi, M.; Edwards, S. F.; Warner, M. *Polymer* **1981**, *22*, 1010–1018.
(35) Klein, P. G.; Ladizesky, N. H.; Ward, I. M. *Polymer* **1987**, *28*, 393–398.
(36) De Rosa, M. E.; Winter, H. H. *Rheol. Acta* **1994**, *33*, 220–237.
(37) Treloar, L. R. G. In *The Physics of Rubber Elasticity*, 3rd ed.; Oxford University Press: New York, 1975; pp 74−75.
(38) Kapnistos, M.; Lang, M.; Vlassopoulos, D.; Pyckhout-Hintzen, W.; Richter, D.; Cho, D.; Chang, T.; Rubinstein, M. *Nat. Mater.* **2008**, *7*, 997–1002.
(39) Williams, M. L.; Landel, R. F.; Ferry, J. D. *J. Am. Chem. Soc.* **1955**, *77*, 3701–3707.
(40) Schmidt, A. *Macromol. Rapid Commun.* **2006**, *27*, 1168–1172.